Novel Morphology Evolution in Thick Films of a Polymer Blend

Matthew Moffitt, Yahya Rharbi, Huxi Li, and Mitchell A. Winnik*

Department of Chemistry, University of Toronto, 80 St. George Street, Toronto, Ontario M5S 3H6, Canada

Received September 26, 2001
Revised Manuscript Received February 26, 2002

Over the past decade, the behavior of phase-separating binary polymer mixtures in thin films ($\leq 1\ \mu$m) has generated interest among both theoreticians[1−7] and experimentalists.[8−17] In systems undergoing spinodal decomposition, the preferential attraction of one component to either or both of the surfaces of a thin film results in a break in the normal symmetry. Rather than isotropic percolating structures, concentration waves normal to the surface develop, forming a laminar phase morphology. This phenomenon has been termed "surface-directed spinodal decomposition". Investigations of surface effects on phase separation and coarsening in thick polymer films ($\gg 1\ \mu$m) are less common,[18−20] as surface asymmetries are expected to give way to bulk phase separation at large distances from the surface. However, the coatings industry has invested some effort into the study of thick films of self-stratifying coatings, which are complex formulations of incompatible polymers, pigments, and solvent mixtures.[21−25] Such films develop bilayer and multilayer structures as the coatings are dried, due to a combination of phase separation and surface effects.

The vast majority of work on surface-directed spinodal decomposition has been carried out using model binary systems with well-defined one- and two-phase behavior over a range of temperatures and compositions. In this communication, we wish to report surprising surface-directed phase evolution in moderately thick films of a ternary blend containing two semicrystalline polymers: namely, polypropylene (PP), polyethylene (PE), and an ethylene−propylene copolymer (EPR), blended at a weight ratio of PP/PE/EPR = 81/14/5. The latter component (EPR) serves as a compatibilizer for the other two components, which are highly immiscible at all temperatures and compositions.[26] Such thermoplastic olefin (TPO) blends have a number of industrial applications, including plastics recycling[27] and the fabrication of automotive parts.[28,29] We annealed films (thickness = ca. 100 μm) of the PP/PE/EPR blend above the melting point in a stainless steel mold and found phase-evolution behavior that bears certain similarities to surface-directed spinodal decomposition in thin films, including a laminar structure and evidence of hydrodynamic flow.

The polymers used to produce the blend were PP from Eastman (M_w = 164 000, M_n = 46 900), linear low-density PE from Dupont Canada (M_w = 35 900, M_n = 12 200), and EPR from Bayer (E/P = 70/30; M_w = 346 600, M_n = 126 100). Blending was carried out by codissolving the three components in hot *m*-xylene (polymer concentration 1.1 wt %) followed by precipitation into acetone.[30] Prior to blending, the EPR component had been labeled with a small amount of the dye

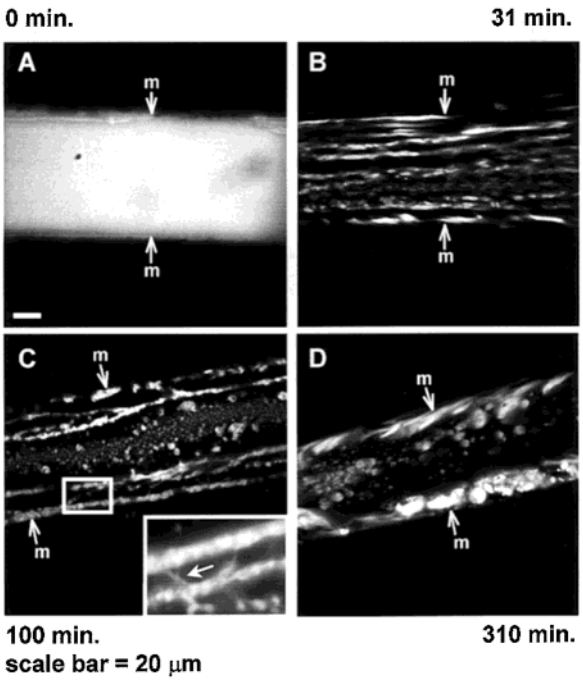

Figure 1. LSCFM images of PP/PE/HY-EPR (81/14/5) films for different annealing times at 175 °C (A, 0 min; B, 31 min; C, 100 min; D, 310 min). The top and bottom surfaces of the film, which were in contact with the mold during annealing, are indicated "m" in the figure. The inset shows an enlargement of the region between the outer layers of high concentration after 100 min annealing. "Channels" between the layers, which allow hydrodynamic draining of PE and HY-EPR to the surface of the film, are visible (arrow).

HY-NH_2 via succinic anhydride groups on the copolymer to provide contrast for laser scanning confocal microscopy (LSCFM); the copolymer in the blend is therefore designated HY-EPR. The labeling procedure will be detailed in a future paper.[31] Precipitation of the blend into acetone is effectively a "deep quench" into the spinodal region of the phase diagram, although the demixing process is rapidly frozen by crystallization of PP and PE. To obtain 100 μm thick films of the blend, the powder was pressed at 150 °C under 2 metric tons for 90 s and then rapidly quenched in cold water. These films were sandwiched between two polished, stainless steel plates that had been previously coated with very thin films of the paraffin oil Sunpar-120 (mold-release agent). The plates and film were then placed in a preheated mold and allowed to reach the equilibrium temperature of 175 °C (above M_p of PP and PE). Morphology evolution in the melt state was followed by annealing the film within the mold for different times before rapid quenching in cold water.

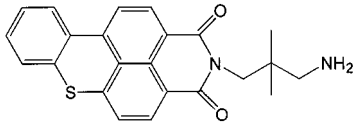

HY-NH_2

Cross sections of a series of blend films annealed for different times are shown in Figure 1. The top and bottom surfaces of the films, which were in contact with

10.1021/ma011679+ CCC: $22.00
Published on Web 03/29/2002

the stainless steel mold plates during annealing, are indicated "m" in the figure. In these LSCFM images, white regions indicate the locus of fluorescently labeled HY-EPR within the blend. Our work on PP/PE/HY-EPR ternary blends has shown that this EPR (E/P = 70/30) is partially soluble within the PE phase: as PE and HY-EPR demix from the PP major phase, HY-EPR encapsulates the PE phase, penetrating the PE domains while concentrating at the interphase.[31] Therefore, along with acting as a compatibilizer, HY-EPR serves as a "tracer" for the PE phase in LSCFM experiments, albeit a tracer that plays a distinct role in the kinetics of phase separation.[26,31] For this reason, we refer to the white phase collectively as the PE/HY-EPR (minor) phase and the black phase as the PP (major) phase.

Without any annealing (Figure 1A), the film appears uniformly fluorescent, indicating that precipitation into acetone and subsequent pressing led to domains too small to be resolved at this magnification. Figure 1B reveals a remarkable evolution in the phase morphology after only 31 min in the melt state. A quasi-periodic, or laminar, phase morphology is clearly visible, with concentrated PE/HY-EPR layers at both surfaces of the mold and alternating concentration and depletion layers (white and black, respectively) running parallel to the surfaces. This laminar morphology is reminiscent of surface-driven spinodal decomposition in thin films, in which composition waves radiate from the surface, as a result of the competition between surface wetting and isotropic χ-dependent thermal fluctuations.[1,4,8,10] To our knowledge, this is the first time that a laminar structure of this type has been observed as a result of phase evolution in such a thick film. Additional similarities to thin-film spinodal decomposition are found when we consider further annealing of the blend (t = 100 min, Figure 1C). Here, the high-concentration layers near the surfaces have coarsened at the expense of the inner layers, leaving a region of intermediate PE/HY-EPR composition in the center of the film made up of small particles of the minor phase. We find this stage of phase evolution to resemble closely the four-layer to bilayer transition that has been observed in thin-film surface-directed spinodal decomposition, in which material from an inner concentration layer is eventually transferred to a wetting layer at the surface.[16] It appears that preferential wetting of the mold surfaces by the PE/HY-EPR phase is a driving force in the phase evolution of the present system. The eventual formation of a single 15−20 μm thick concentration layer of PE/HY-EPR at each of the mold surfaces (Figure 1D, t = 310 min) supports this conclusion.

The mechanism of mass transport in the late stages of surface-directed spinodal decomposition is a critical factor in understanding phase evolution in such systems. A growing number of theoretical studies have predicted hydrodynamic draining[32] of the wetting component toward the surface,[5,6] accounting for t^1−$t^{1.5}$ growth of the wetting layer.[10,11,15−18] This process occurs via channels of the wetting component which penetrate the depletion layers, allowing material to flow through the channels.[16] To date, direct experimental evidence for the existence of these channels is rare and has been limited to the observation of perforations in the top layer of thin films by AFM.[11,15,16] In Figure 1C (inset), we show what we believe to be the first image of hydrodynamic channels connecting two concentration layers and the first evidence of hydrodynamic channels in a thick film. It appears that draining of material through such channels results in the evolution of phase morphology between t = 100 and 310 min (Figure 1, C and D, respectively). We will presently discuss top-view images of these films, which show a network of channels between concentration layers after 31 min of annealing. This observation suggests that phase evolution between t = 31 and 100 min is also governed by hydrodynamic flow.

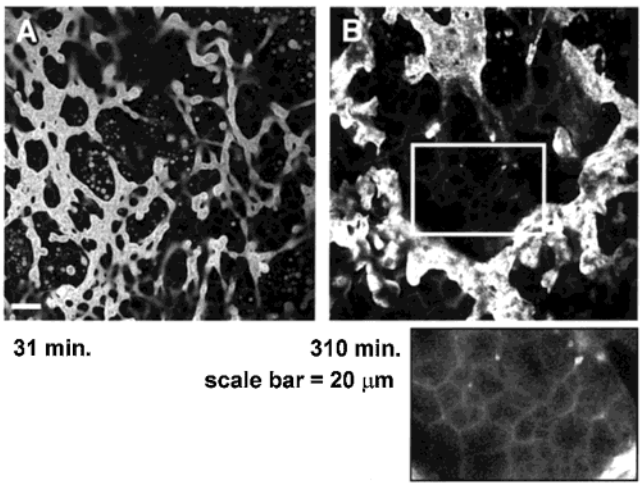

Figure 2. LSCFM images of the PP/PE/HY-EPR (81/14/5) film surface (top view) after (A) 31 min and (B) 310 min annealing at 175 °C. After 31 min annealing (A), a coarse network of PE/HY-EPR is shown to extend in a two-dimensional sheet parallel to the surface. Such sheets correspond to the alternating layers of high concentration visible in Figure 1B. A much finer network is also visible, believed to be channels through which material flows between layers during annealing. After 310 min annealing (B), the film surface consists of large islands of PE/HY-EPR with less connectivity than the coarse 2D network at earlier times. The fine, highly connected network of channels is still visible, which is shown enlarged and with improved contrast in the inset.

LSCFM images of the top mold surface of the blend films after 31 and 310 min in the melt state are shown in Figure 2. Figure 2A shows a coarse network of the PE/HY-EPR phase along with coexisting core−shell particles. Also visible is a fainter and much finer network of the minor phase. A series of optical sections taken at increasing distances from the surface (not shown) suggest that the coarse network is not isotropic and grows preferentially in sheets running parallel to the surface. It therefore appears that these two-dimensional sheets of the minor phase are responsible for the alternating concentration and depletion layers observed in Figure 1B. Core−shell particles are found to be distributed isotropically within the film, both within and between the two-dimensional sheets. From optical sectioning at various depths, the finer network appears to have an isotropic structure in three dimensions, which suggests that it is a network of the aforementioned hydrodynamic channels, connecting two-dimensional sheets of the coarser network throughout the film. After 310 min annealing (Figure 2B), the film surface consists of a noncontinuous wetting layer made up of large islands of PE/HY-EPR. These islands show less connectivity in two dimensions than the coarse network at earlier times. The fine, highly connected network of channels is still visible (Figure 2B, inset), and this extends in three dimensions throughout the film.

Hashimoto et al. have recently observed anisotropic sheets of a percolating phase running parallel to the surface in thick films of polybutadiene/polyisoprene sandwiched between glass plates.[20] (Unlike in the present work, they did not observe alternating concentration and depletion layers starting at the film surfaces.) These authors attributed the phenomenon to a heterogeneous percolation-to-cluster transition (PCT) in which the glass surfaces induce anisotropy in the phase morphology. They proposed that the blend consists of a 3D percolating phase before the PCT, which "breaks" in the direction normal to the surface faster than along the parallel direction. A similar model, combined with the idea of surface wetting, may be used to explain the interesting evolution of morphologies in the present thick film: During precipitation of the blend, spinodal decomposition of the blend should occur isotropically, forming a 3D percolating network of PE/HY-EPR that extends throughout the thick film; prior to annealing, the features of this network are too small to be resolved by LSCFM. Preferential attraction of PE/HY-EPR to the mold surfaces may then induce material flow through the network, which competes with the isotropic breakdown of the network into clusters or particles (PCT), causing particles and network to coexist. Within the network, hydrodynamic flow induces anisotropic coarsening of the network in 2D sheets, eventually draining these sheets into a single wetting layer at each surface. Along with explaining the observed similarities with surface-directed spinodal decomposition in thin films (concentration and depletion layers, hydrodynamic flow), this model also accounts for the important differences, including a much coarser structure and a greater number of layers in the present system. Such differences may arise from the fact that, in thin films, the effect of the surface is felt from the very early stages of spinodal decomposition. In contrast, for the present case of thick polyolefin films, surface anisotropy does not come to bear until after the phase compositions have been well established. The morphology evolution seen in Figure 1 may therefore be more a consequence of surface-directed coarsening than a surface effect on demixing.

Finally, we have further demonstrated the importance of the mold surface by annealing a film of the PP/PE/HY-EPR blend with one surface in contact with a 15 μm film of homo-PP (Escorene 1042, Exxon) and the other in direct contact with the mold (Figure 3). Rather than material flow toward both surfaces (as in Figure 1D), the cross section of the film (Figure 3A) clearly shows that PE/HY-EPR has drained away from the lower energy PP surface (top) toward the higher energy mold surface (bottom), forming a thick (30−40 μm) wetting layer consisting of coarse particles. Between this wetting layer and the PP film (inset), a PE/HY-EPR concentration gradient is visible, as are hydrodynamic channels extending down into the wetting layer (arrow). A top-view of this region (Figure 3B) shows that the channels make up a percolating network. As a result of material flow through these channels, the concentration of PE/HY-EPR increases gradually toward the metal surface, followed by a sharp transition to the high-concentration wetting layer. This transition can be described as a space-dependent PCT, caused by a concentration gradient extending from one surface to the other.

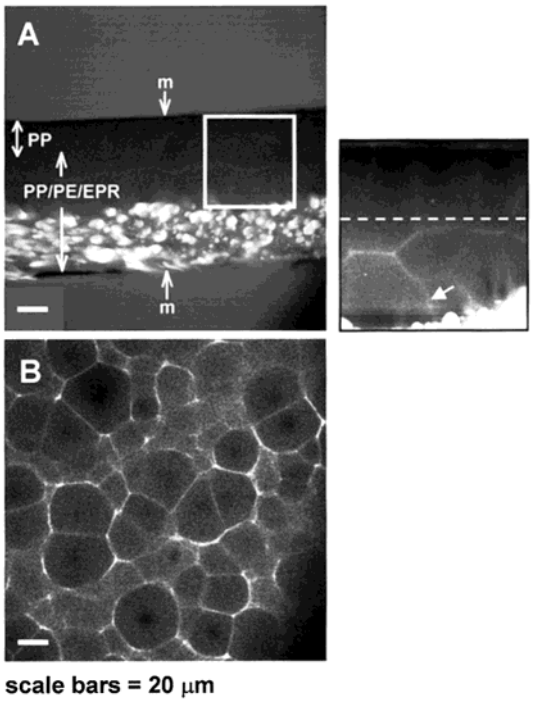

Figure 3. LSCFM images of a PP/PE/HY-EPR (81/14/5) film annealed for 310 min at 175 °C, with the top surface in contact with a thin film of homo-PP and the bottom surface directly in contact with the mold. From the cross section (A), it can be seen that wetting of the mold surface drives PE and HY-EPR to the bottom of the film, where a thick (30−40 μm) wetting layer is found. The inset shows the PE/HY-EPR gradient region and a network of channels extending down to the wetting layer (arrow). The dotted line in the inset shows the optical plane corresponding to the top view of the network (B).

In conclusion, we have demonstrated novel morphology evolution in thick films of PP/PE/HY-EPR during annealing, driven by preferential wetting of the mold surface. This phenomenon bears many similarities to surface-directed spinodal decomposition in thin films, but with a coarser structure and a greater number of layers. Morphology evolution by this mechanism may have important applications in such areas as solvent-free self-stratifying coatings and the preparation through processing of novel anisotropic materials.

Acknowledgment. The authors thank Materials and Manufacturing Ontario (MMO) for support of this research and Dr. Hayder Zahalka (Bayer) for providing the EPR sample. We also thank Dr. Rose Ryntz (Visteon) for helpful discussions.

References and Notes

(1) Ball, R. C.; Essery, R. L. H. *J. Phys.: Condens. Matter* **1990**, *2*, 10303.
(2) Puri, S.; Binder, K. *Phys. Rev. A* **1992**, *46*, 4487−4489. Puri, S.; Binder, K.; Frisch, H. L. *Phys. Rev. E* **1997**, *56*, 6991−7000.
(3) Brown, G.; Chakrabarti, A. *Phys. Rev. A* **1992**, *46*, 4829−4835.
(4) Marko, J. F. *Phys. Rev. E* **1993**, *48*, 2861−2879.
(5) Chen, H.; Chakrabarti, A. *Phys. Rev. E* **1997**, *55*, 5680−5688.
(6) Tanaka, H.; Araki, T. *Europhys. Lett.* **2000**, *51*, 154−160.
(7) Bastea, S.; Puri, S.; Lebowitz, J. L. *Phys. Rev. E* **2001**, *63*, 041513-1−041513-7.
(8) Jones, R. A. L.; Norton, L. J.; Kramer, E. J.; Bates, F. R.; Wiltzius, P. *Phys. Rev. Lett.* **1991**, *66*, 1326−1329.
(9) Bruder, F.; Brenn, R. *Phys. Rev. Lett.* **1992**, *69*, 624−627.

(10) Krausch, G.; Mlynek, J.; Straub, W.; Brenn, R.; Marko, J. F. *Europhys. Lett.* **1994**, *28*, 323−328. Krausch, G.; Dai, C.-A.; Kramer, E. J.; Bates, F. S. *Phys. Rev. Lett.* **1993**, *71*, 3669−3672. Krausch, G.; Dai, C.-A.; Kramer, E. J.; Marko, J. F.; Bates, F. S. *Macromolecules* **1993**, *26*, 5566−5571.
(11) Jandt, K. D.; Heier, J.; Bates, F. S.; Kramer, E. J. *Langmuir* **1996**, *12*, 3716−3720.
(12) Affrossman, S.; Henn, G.; O'Neill, S. A.; Pethrick, R. A.; Stamm, M. *Macromolecules* **1996**, *29*, 5010−5016.
(13) Sung, L.; Karim, A.; Douglas, J. F.; Han, C. C. *Phys. Rev. Lett.* **1996**, *76*, 4368−4371.
(14) Genzer, J.; Kramer, E. J. *Phys. Rev. Lett.* **1997**, *78*, 4946−4949.
(15) Wang, H.; Composto, R. J. *J. Chem. Phys.* **2000**, *113*, 10386−10397.
(16) Rysz, J.; Ermer, H.; Budkowski, A.; Bernasik, A.; Lekki, J.; Juengst, G.; Brenn, R.; Kowalski, K.; Camra, J.; Lekka, M.; Jedlinski, J. *Eur. Phys. J. E* **2001**, *5*, 207−219. Rysz, J.; Bernasik, A.; Ermer, H.; Budkowski, A.; Brenn, R.; Hashimoto, T.; Jedlinski, J. *Europhys. Lett.* **1997**, *40*, 503−508.
(17) For film thicknesses < 0.2 μm, see: Keblinski, P.; Kumar, S. K.; Maritan, A.; Koplik, J.; Banavar, J. R. *Phys. Rev. Lett.* **1996**, *76*, 1106. Sung, L.; Karim, A.; Douglas, J. F.; Han, C. C. *Phys. Rev. Lett.* **1996**, *76*, 4368. Karim, A.; Slawecki, T. M.; Kumar, S. K.; Douglas, J. F.; Satija, S. K.; Han, C. C.; Russell, T. P.; Liu, Y.; Overney, R.; Sokolov, J.; Rafailovich, M. H. *Macromolecules* **1998**, *31*, 857.
(18) Cumming, A.; Wiltzius, P.; Bates, F. S.; Rosedale, J. H. *Phys. Rev. A* **1992**, *45*, 885−897.
(19) Li, L.; Sosnowski, S.; Chaffey, C. E.; Balke, S. T.; Winnik, M. A. *Langmuir* **1994**, *10*, 2495. Li, L.; Sosnowski, S.; Kumacheva, E.; Winnik, M. A. *Langmuir* **1996**, *12*, 2141−2144.
(20) Takeo, H.; Nakamura, E.; Hashimoto, T. *J. Chem. Phys.* **1999**, *110*, 3612−3620.
(21) Funke, W. *J. Oil Colour Chem. Assoc.* **1976**, *59*, 506.
(22) Verkholantsev, V. V. *Prog. Org. Coat.* **1995**, *26*, 31.
(23) Verkholantsev, V.; Flavian, M. *Prog. Org. Coat.* **1996**, *29*, 239.
(24) Carr, C.; Wallstom, E. *Prog. Org. Coat.* **1996**, *28*, 161. Walbridge, D. J. *Prog. Org. Coat.* **1996**, *28*, 155. Benjamin, S.; Carr, C.; Walbridge, D. J. *Prog. Org. Coat.* **1996**, *28*, 197. Toussaint, A. *Prog. Org. Coat.* **1996**, *28*, 183.
(25) Ming, W.; Laven, J.; van der Linde, R. *Macromolecules* **2000**, *33*, 6886.
(26) Li, L.; Chen, L.; Bruin, P.; Winnik, M. A. *J. Polym. Sci., Part B: Polym. Phys.* **1997**, *35*, 979−991.
(27) Teh, J. W.; Rudin, A.; Keung, J. C. *Adv. Polym. Technol.* **1994**, *13*, 1−23.
(28) Ryntz, R. A.; Ramamurthy, A. C.; Holubka, J. W. *J. Coat. Technol.* **1995**, *67*, 23.
(29) Tong, J.; Moffitt, M.; Huang, X.; Winnik, M. A.; Ryntz, R. A. *J. Polym. Sci., Part A: Polym. Chem.* **2001**, *39*, 239−252.
(30) Inaba, N.; Sato, K.; Suzuki, S.; Hashimoto, T. *Macromolecules* **1986**, *19*, 1690−1695.
(31) Moffitt, M.; Rharbi, Y.; Li, H.; Winnik, M. A., to be published. (For details of a similar procedure for the labeling of an ethylene−butene copolymer, see ref 23.)
(32) Siggia, E. D. *Phys. Rev. A* **1979**, *20*, 595−605.

MA011679+